Materials and Structures (2009) 42:1101–1116
DOI 10.1617/s11527-008-9446-y

ORIGINAL ARTICLE

Compression behaviour of non-industrial materials in civil engineering by three scale experiments: the case of rammed earth

Quoc-Bao Bui · Jean-Claude Morel · Stéphane Hans · Nicolas Meunier

Received: 17 June 2008 / Accepted: 10 October 2008 / Published online: 30 October 2008

Abstract In order to give an example of a scientific approach adapted to non-industrial materials, we chose to study a structural element: a load-bearing building wall made of rammed earth material. Rammed earth construction is an ancient technique which is attracting renewed interest throughout the world today. Although rammed earth is currently regarded as a promising material in the construction sector in the context of sustainable development, it is still difficult to quantify its durability, as well as its thermal and mechanical performances, which discourages people from using it. This paper is devoted to the study of the last problem. Three different scales were studied. The first is the scale of in-situ walls. Dynamic measurements were carried out on site to determine the Eigen frequencies of the walls. The elastic modulus was determined from the frequencies measured by using a finite element model. The second is the scale of a representative volume element (RVE). Rammed earth RVE samples with dimensions similar to those of the walls on site were manufactured and tested in the laboratory. Finally, at the last scale, called the micro-mechanical scale, tests were performed on equivalent compressed earth blocks (CEBs), which can replace the rammed earth RVE samples to facilitate laboratory tests.

Keywords Sustainable development · Rammed earth · Elastic modulus · Vibration · In-situ testing · Compressed earth block

Q.-B. Bui · J.-C. Morel · S. Hans
Université de Lyon, Lyon 69003, France

Q.-B. Bui · J.-C. Morel (✉) · S. Hans
Département Génie Civil et Bâtiment, Ecole Nationale des Travaux Publics de l'Etat, CNRS, URA 1652, 3 rue Maurice Audin, Vaulx-en-Velin 69120, France
e-mail: morel@entpe.fr

N. Meunier
6 rue de l'Eglise, 42170 Chamble, France

1 Introduction

The non-industrial materials used in civil engineering are materials manufactured and installed by masons, with short production cycles. They are usually local materials, i.e. earth, stone, plant fibers mixed with a binder, etc., found on or near a construction site.

Their study and use have become promising in highly industrialised countries for three reasons. The first is the desire for more sustainable development. These materials imply a predominance of human know-how, thus avoiding their replacement by machines. The social aspect is therefore favorable, as is the environmental aspect due to their low embodied energy and transport [1], their safety, durability [2], ability to be re-used, abundance, etc. Finally, in highly industrialised countries the economic aspect remains the most negative but is

evolving positively due to the increase in world population and fossil fuel prices [3]. In developing countries, this last point (the economic aspect) is a favorable one for these materials, which are cheaper than industrial products.

The second point is that structures made of non-industrial materials are still very widespread around the world and even in highly industrialised countries, despite much destruction. For example, there are about 9000 km of dry stone retaining walls along the UK road network alone, with an estimated replacement value in excess of 1.4 billion euros. In France, there were about 2.4 million earthen houses in 1987 [4]. Their maintenance, often more than a century after their construction, poses technical and financial problems, since it is performed empirically, without scientific data.

The third reason is the desire to strengthen protection from natural risks such as floods and earthquakes and to cope with anthropic environmental changes that have not been taken into account by empiricism, such as climate change. This requires assessing the relevance of these materials and structures with respect to modern safety conditions, i.e. with an appropriate and reliable scientific tool.

The "modern" materials composing civil engineering structures are optimised with industrial processes that are often standardised, in order to fulfill a specific function for a limited time. Therefore one superimposes different materials to achieve an effective complex constructive system responding to a physical and social demand. Most often, one seeks very high performance from the component without worrying about other aspects. The weakness of these systems is their uncontrolled long-term behaviour and their reuse, which is sometimes even dangerous (asbestos for example).

The non-industrial materials used in construction are the result of an empirical optimisation over a thousand years old. These local materials and the structures made with them vary widely in each building due to the variability of geological sites and the fact that they are not produced using a standardised industrial process. The soil of the site is the material used to meet all immediate needs [5], for example, in the case of a wall: health, durability, hygrothermal comfort, mechanical stability, isolation.

Material optimisation does not target a single area, for example compressive strength, but is a compromise between many criteria. For example, in the case of rammed earth or stone masonry, the thickness of the wall is at least 50 cm to ensure correct hygrothermal behaviour. With such thicknesses, the compression safety factors are around 10. The complexity will be to adapt to the variability of the material and not the difficulty to obtain a performance. Therefore, from a scientific viewpoint, it is not desirable to use very sophisticated rheological laws, very expensive to use, but rather performance measurement methods giving reliable results and usable in practice even if not very precise. Thus, emphasis is placed on developing test methods that can characterise these materials. Next, the objective is to quantify the behaviour of these materials and then the behaviour of structures they form.

2 Rammed earth

As an example of a scientific approach adapted to non-industrial materials, we chose to study a structural element: a load-bearing building wall made of rammed earth material. The rammed earth is a clayey soil (earth) compacted into a formwork. The earth composition varies greatly but contains no organic component and enough clay, which acts as a binder between the grains, a mixture of silt, sand, gravel and stones with a diameter of a few centimeters. Compaction is performed using a water content considered optimum, i.e. that provides the highest dry density for a fixed compaction energy. This process is called the dry method because the water content is around 10%, while a paste should have a water content of about 25%. The rammed earth is composed of several layers of earth. The earth is poured in layers about 15 cm thick into a formwork (wooden or metal). It is rammed with a rammer (manual or pneumatic). After compaction, the thickness of each layer is 8–10 cm. The procedure is repeated until completion of the wall.

For traditional rammed earths, the only binder is clay, they are referred to as "unstabilised rammed earth". With industrialisation, modern rammed earths appeared in which other binders were added, such as cement, hydraulic or calcium lime. They are called "stabilised rammed earth". The main advantage of stabilising the rammed earth is to increase its durability (with respect to water attack) and mechanical performance (compressive strength).

This paper presents a study on quantifying the mechanical characteristics of the rammed earth material. We do not consider stabilised rammed earth as an objective to be pursued for several reasons. The first is linked to durability. A study on rammed earth walls exposed for 20 years to natural conditions on site was carried out [2]. The result of erosion measurements using the stereophotogrammetric method shows that traditional unstabilised rammed earth, subjected to the climate studied, may reach a lifetime much longer than 60 years. In France and Europe, a huge stock of unstabilised rammed earth houses remain that have exceeded a hundred years in age. We can therefore trust unstabilised rammed earth if its manufacture is well performed and controlled. The second reason is economic. Stabilisers (cement or lime) obviously increase construction costs, and in addition are not always available (in remote areas or in countries where one must import these products). The third reason is the environmental impact in the demolition phase. While unstabilised rammed earth can be reused quite easily, recycling of stabilised rammed earth becomes very difficult or even impossible.

3 The laboratory manufacturing process for a representative volume element (RVE) of rammed earth

Still too little scientific research [6–10] has been conducted on the mechanical behaviour of rammed earth (especially unstabilised rammed earth) to characterise its compression strength and elastic modulus. One of the main difficulties of laboratory studies is the manufacturing process used to make representative rammed earth samples. The first problem with laboratory manufacturing is to determine the manufacturing water content and the compaction energy representing those of in-situ rammed earth. Because in-situ rammed earth is manufactured manually, the compaction energy depends on the practices of each mason, even if he uses the same rammer. It is therefore difficult to propose an effective laboratory method to determine the representative water content corresponding to a representative compaction energy.

Sample size is another element to consider when manufacturing representative samples of in-situ material. The first point that should be considered is the material grain size. The sample dimensions must be sufficient for the test to be homogeneous at the considered scale. Moreover, the sample dimensions influence the compaction energy transmitted to the rammed earth: the effect of friction with the formwork, the number of superimposed blows. In addition, rammed earth is not a homogeneous material at the decimeter scale. It consists of several layers and in each layer, a material density gradient is observed. The upper portion of a layer, directly in contact with the rammer during compaction, is denser, while the lower portion, not affected by the rammer, is less dense (Fig. 1c). This complexity must also be taken into account when manufacturing representative rammed earth samples.

Some studies focus on the mechanical behaviour of unstabilised rammed earth [6–10]. The results of these studies are presented in Table 1. However, they have not yet dealt with the difficulties presented above concerning the manufacture of representative rammed earth samples. First, in these studies, the authors used the heavy Proctor test to determine the optimum water content for laboratory manufacture, without showing the correlation between the compaction energy of this test and that of in-situ rammed earth. Secondly, the samples studied in most of these studies [6–8] are just small samples manufactured in a laboratory and thus not very representative of in-situ material. In the study by Jaquin et al. [9], dry density is not presented, making it impossible to compare it with other studies. In addition, it should be noted that the samples with a low slenderness ratio (the cases of [6, 7]) do not give direct results. This is why Hall and Djerbib [6] used a correction factor of 0.7 for their compressive strength results in their study. The relevency of such factor for compacted earth is discussed in Morel et al. [11]. The study of Maniaditis and Walker [10] showed the difference of results obtained from small samples and those of real scale samples. However, in all of these studies, no comparison of the laboratory results with those of in-situ rammed earth was made.

One solution that can avoid the difficulties of laboratory manufacturing is to take samples on site. Sample taking from in-situ walls with a chainsaw was attempted [12]. However, this method encounters many difficulties with a material such as rammed earth. The disadvantages are vibration generation and the use of water during cutting, which can reduce

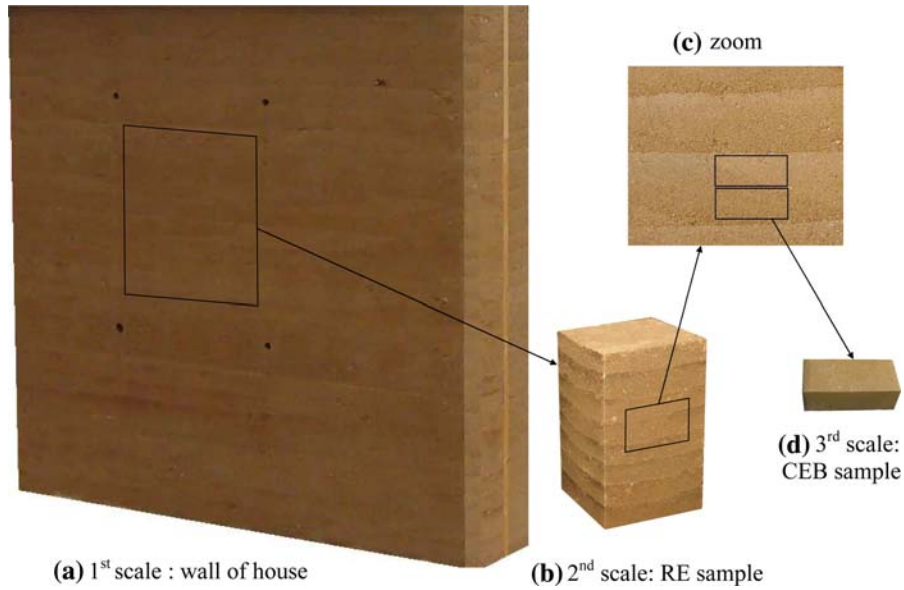

Fig. 1 Three scales of study

Table 1 Summary of papers on rammed earth mechanical characteristics

Study	d (kg/m^3)	R_c (MPa)	$E_{tangent}$ (MPa)	Sample dimensions (cm)	Slenderness
Hall [6]	2020–2160	0.75–1.46[a]	Not measured	Cubes 10	1
Lilley [7]	1870–2170	1.8–2.0	Not measured	Cubes 15	1
Maniatidis [8]	1850	3.88	205	$d = 10$, $h = 20$	2
Jaquin [9]	Not presented	0.6–0.7	60	$\approx 100 \times 100 \times 30$	3.3
Maniatidis [10]	1850	2.46	160	$d = 10$, $h = 20$	2
	1763–2027	0.62–0.97	60–70	$30 \times 30 \times 60$	2

[a] Value corrected because of the very low slenderness

sample strength, particularly due to the separation of the earth layers.

4 Adopted procedure

The study presents three approaches at three different test scales (Fig. 1) to the measure elastic moduli of rammed earth.

The first is on the scale of an in-situ wall. Dynamic measurements were carried out on site to determine the Eigen frequencies of the walls. The elastic modulus was determined from the frequencies measured by using a finite element model.

A rammed earth house under construction near Thiers (France) was chosen as the subject of the study, Figs. 2 and 3. It should be noted that the architecture is modern but the material is fairly similar to that of old houses. The grain size distribution of the earth is presented in Fig. 4. Metal formworks and a pneumatic rammer were used. The rammed earth walls 2.3 m in height were built on 0.3 m of concrete base paved with stones. The advantages of a house under construction are multiple: we can perform the measurements on the rammed earth walls alone, without roof elements or other structural links, therefore the results enable us to obtain the elastic modulus of the rammed earth itself, without any influence from other elements. Secondly, walls under construction are not yet completely dry, so we can observe the changes in their characteristics over time, particulary the loss of moisture content, by taking several measurements at different moments.

The second approach is on the scale of a representative volume element (RVE). Samples were manufactured by the same mason who built the rammed earth house presented above. The sample

Fig. 2 Rammed earth house under construction, at the time of the first measurements, in June 2006

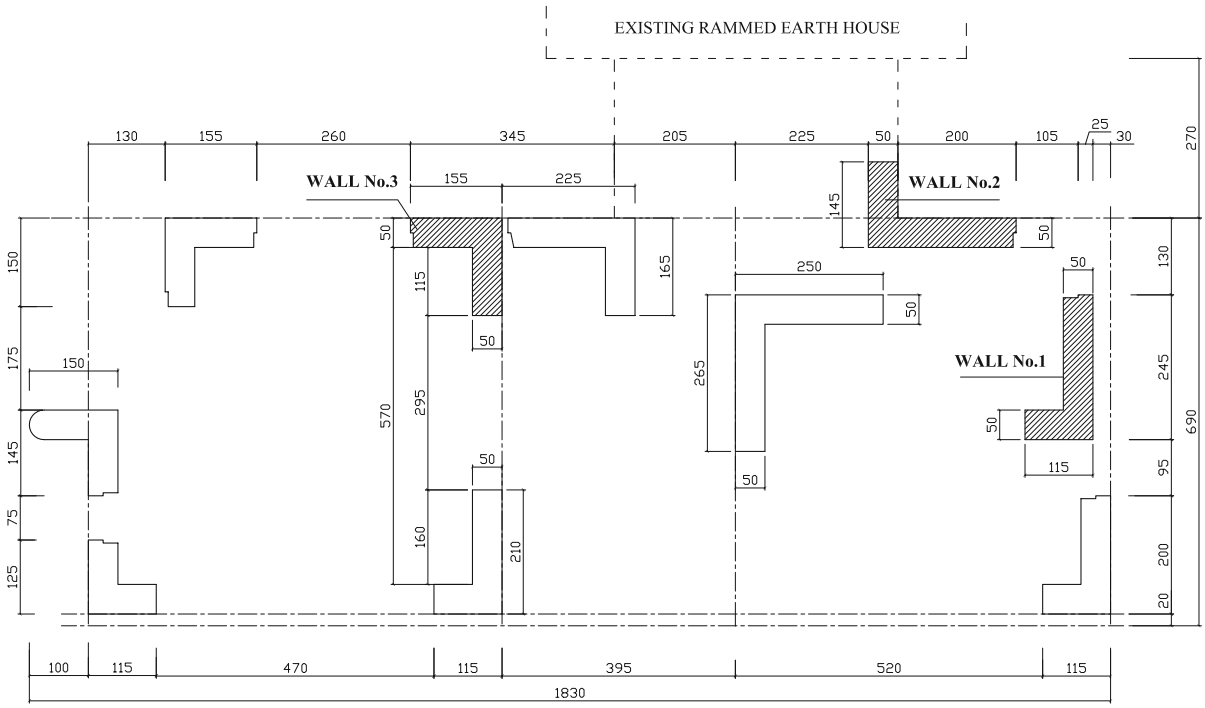

Fig. 3 Plan of the rammed earth walls of the house and the location, dimensions (in cm) of the walls measured (No. 1, 2 and 3)

dimensions were close to those of the in-situ walls. Earth was also taken from the site and transported to the laboratory. Therefore the samples could provide a good representation of the in-situ wall material. The elastic modulus and compressive strength of the samples were determined using unconfined compression tests in the laboratory.

Finally, with regard to the last micromechanical scale approach, tests were performed on equivalent CEBs (Fig. 1d), which can replace the rammed earth samples to facilitate the laboratory test procedure.

5 Measurements at a RVE scale—laboratory samples

We will start with the second scale (Fig. 1b) since this approach is classic in Continuum Mechanics.

5.1 Laboratory manufacturing process

The manufacture of laboratory samples must ensure a faithful representation of the in-situ wall material. The manufacturing mode and material used should be

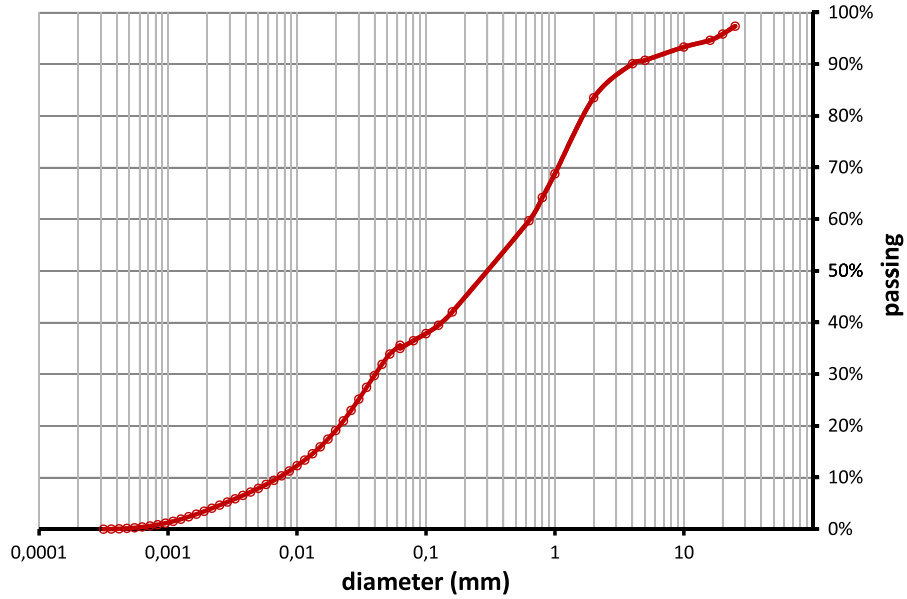

Fig. 4 Grains size distribution curve of the earth used

Fig. 5 Left: (40 × 40 × 65) cm^3 sample manufactured in the laboratory, surfaced on top with cement mortar. Right: cylindrical sample 16 cm in diameter × 26.5 cm high

as identical as possible to those used for the house. The earth was taken from the construction site of the measured house presented above. The mason who manufactured the laboratory samples was the same one who built the house. His equipment (metal formwork, pneumatic rammer) were the same as those used on site. Finally, the manufacturing water content in the laboratory was the same as that on site. All these conditions ensure the same compaction energy, and therefore, the same density. The compaction energy obtained by rammed earth is influenced by the sample size, which is why the sample dimensions are also similar to those of in-situ walls: 3 samples with dimensions of (40 × 40 × 65) cm^3 (Figs. 1 and 5 on the left) were manufactured. We did not manufacture samples 50 cm thick like the in-situ walls, since it would then have been impossible to place the samples on the press for the subsequent compression tests.

The manufacturing water content of the earth was about 10%. The sample was manufactured on a rigid metal plate to facilitate transport after manufacture. Surfacing was also performed with a cement mortar to give a flatter surface, but without achieving a perfectly flat surface.

To observe the influence of the sample size, we also manufactured cylindrical samples 16 cm in diameter (Fig. 5 on the right). The cylindrical metal mould was 16 cm in diameter and 32 cm high. The pneumatic rammer was adapted so as to enter directly into the mould. The height of samples obtained was 26.5 cm. Surfacing was also performed with cement mortar.

5.2 Dry density measurements

The samples were weighed before the test. To weigh prismatic samples over 200 kg, an electronic weighing scale was used that was attached to the the metal bottom of the sample with cables, raised the metal bottom and the sample, and then indicated the total weight. The dry density was obtained by subtracting the moisture content. The water content was

calculated from the pieces taken after the compression test. The average dry density obtained was 1900 kg/m^3. The dry densities indicated in other existing studies (such as [6–8]) were only the dry density of small samples manufactured in moulds, and no evidence indicates that they are representative of in-situ rammed earth. The manufacture of 10 cm cubic samples proposed by Hall and Djerbib [6] yielded dry densities from 2020 to 2160 kg/m^3. The difference is due one hand to the difference in the earth used, and also perhaps because in small samples, the thickness of each earth layer is smaller, therefore the earth is denser and more compact. Note that this is not the case of in-situ rammed earths where we always find a density gradient in each earth layer. For the same reason, the cylindrical samples made in our laboratory (Fig. 5 right) are not a good representation of in-situ rammed earth. Their dry densities, compression strength and elastic modulus were higher than those of the prism samples even if it was demanded to the mason to compact as close as possible to the in-situ walls.

Fig. 6 Unconfined compression test of (40 × 40 × 65) cm^3 sample

5.3 Unconfined compression test

The sample (plus the metal bottom) was transported by forklift and placed directly on the lower plate of the press (Fig. 6). The contact between the metal plate placed above the sample and the top plate of the press was articulated. With a 1.6 slenderness ratio of the sample, the friction effect did not play an important role because there was a homogeneous deformed portion in the middle of the sample. The test was controlled by displacement. The loading speed was 0.01 mm/s. We performed several cycles at various load levels, with corresponding stress levels in the sample of 0.06 MPa; 0.12 MPa; 0.22 MPa (samples 1, 2, 3) and 0.4 MPa (only sample 3) respectively (Fig. 7 on the left). The cycles carried out indicate if there is an elasticity of the material and determine the modulus in that case. For each load level chosen, 3 cycles were performed to verify the modulus obtained, Fig. 7 on the right. The first load level corresponds to the stress at the wall base of the in-situ house due to the wall weight itself. The purpose of several load levels is to check if there are changes in elastic modulus at different load levels.

Figure 7 on the left shows a stress–strain curve. The two upper and lower surfaces of the samples were not perfectly flat, thus there was a non-linearity at the beginning portion of the strain–stress curves, because the press plates crushed small elements emerging from the surface despite the surfacing. In the next phase, the stress–strain relationship becomes linear. Let us call the modulus determined in this linear portion of the curve E_{tangent}, conventionally used as the elastic modulus for materials such as steel in the Strength of Materials field.

However, in the case of rammed earth, the elastic portion of the material at the beginning of the test was not yet found. If a preload σ_{preload} is done (in this case σ_{preload} is 0.06, 0.12, 0.22 and 0.4 MPa respectively), the material behaviour becomes almost elastic-linear for the stresses lower than σ_{preload} (Fig. 7 right), which is the hardening phenomenon. During reloading, we measure the elastic modulus, called E_r. Call E_{r1}, E_{r2}, E_{r3}, E_{r4} the reloading moduli corresponding to preloads of 0.06, 0.12, 0.22 and 0.4 MPa, respectively. Then, we notice that there is a modulus change at each preload level. The more the preload σ_{preload} increases, the more the modulus increases (the sample was "consolidated" as in Soil Mechanics). Figure 8 presents the synthesis of the moduli obtained from 3 rammed samples. We assume that the modulus E_r corresponding to $\sigma_{\text{preload}} = 0$ is E_{tangent}.

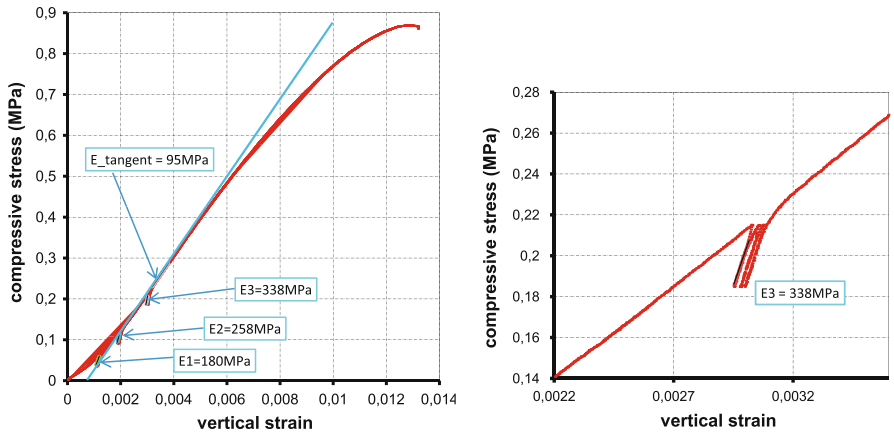

Fig. 7 Strain–stress curve of sample No. 1 ($40 \times 40 \times 65$) cm^3 (left) and zoom of cycles at the third level (right)

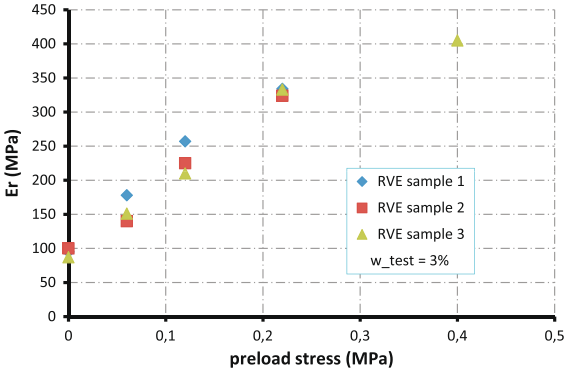

Fig. 8 Synthesis of modulus obtained from 3 rammed samples

6 Micromechanical experiments—CEBs

6.1 Strategy of the approach

Looking at a rammed earth surface, the heterogeneity of this material appears clearly, due not only to stacking of the different layers but also stacking within each layer. In each layer, the upper portion that has directly received the energy compaction during manufacture is denser than the lower portion (Fig. 1c). It is therefore obvious that the upper portion has a higher density than the lower portion.

6.1.1 Adopted hypotheses

In this approach, the following assumptions are made (Fig. 9):

- All layers are *identical* (with thickness e).
- In reality, the dry density decreased continuously from top to bottom within a layer, however, as a first approximation, and in order to work on uniform samples, we assumed that a rammed earth layer consisted of two different homogenous portions: the upper portion with a thickness e_{up}, density d_{up}, corresponding modulus E_{up}, the lower portion with a thickness e_{low}, density d_{low}, and corresponding modulus E_{low}.
- The adhesion between the earth layers is perfect.

6.1.2 Definition of terms

Notes:

- $<d>$ is the representative density of the material at the macroscopic scale.
- $<E>$ is the representative elastic modulus of the material at the macroscopic scale.
- σ is the vertical stress applied in the compression test.

The homogenisation process is classical in the composite materials science [13]. We have the following relationship:

$$\langle E \rangle = \frac{e_{up} + e_{low}}{\frac{e_{up}}{E_{up}} + \frac{e_{low}}{E_{low}}} \quad (1)$$

6.1.3 Strategy of this approach

The strategy of this approach is to manufacture two types of homogenous Compressed Earth Blocks (called CEBs) with the corresponding density d_{up} and d_{low} in Fig. 9 at the top-right. The CEBs are manufactured by a double compaction, which gives samples almost homogenous—isotropic [14, 15]). With an isotropic sample, the loading parallel to the

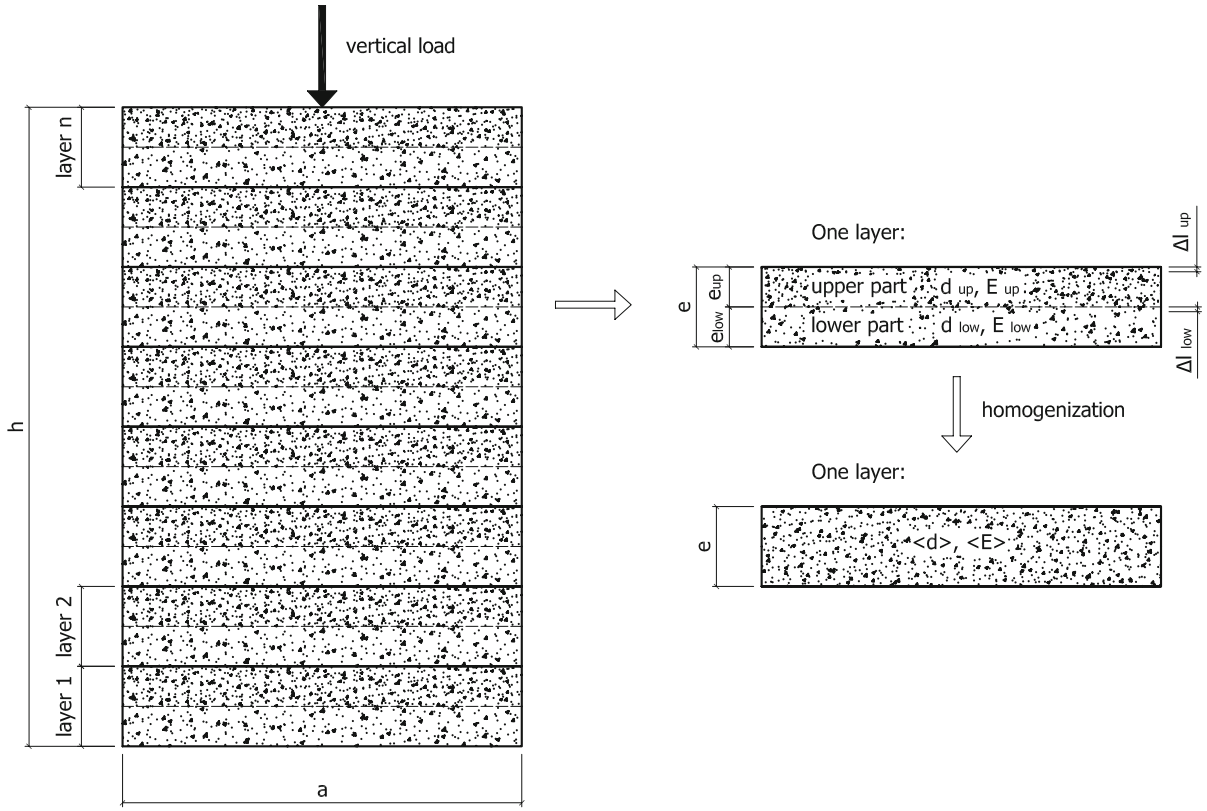

Fig. 9 Left: rammed earth sample at macroscopic scale. Right: microscopic scale on a rammed earth layer and homogenization

longitudinal direction is chosen to limit the problem of friction along the interface between the platen and test specimen. This problem was discussed in Morel et al. [11]. By performing the unconfined compression tests on these CEBs, we can determine the corresponding moduli E_{up} and E_{low}. Using the relationship presented in the Eq. 1, we can determine the equivalent elastic modulus of the rammed earth.

The densities d_{up} and d_{low} can be determined from the laboratory-manufactured rammed earth RVE samples (2nd scale). After the unconfined compression test on prism samples, pieces of layers can be taken fairly easily. Then these pieces are cut into two upper and lower portions with a circular saw. The density of each portion is determined from their weight, volume and moisture content. The volume is determined by measurements in water following the Archimedes' principle, after covering the sample with paraffin.

In cases that we choose reasonably $e_{up} = e_{low}$, we have: $d_{up} = 1980\ \text{kg/m}^3$, which requires that $d_{low} = 1820\ \text{kg/m}^3$ because: $\langle d \rangle = \frac{1}{2}(d_{up} + d_{low}) = 1900\ \text{kg/m}^3$.

Replacing $e_{up} = e_{low}$ in Eq. 1, we obtain:

$$\langle E \rangle = \frac{2 \cdot E_{up} \cdot E_{low}}{E_{up} + E_{low}} \tag{2}$$

6.2 Unconfined compression tests on CEBs

Unconfined compression tests were performed on Compressed Earth Blocks (CEBs), i.e. earth blocks compacted with a manual double compaction press. The earth used to manufacture the CEBs was that of the rammed earth, without stones larger than 3 cm. The CEB dimensions were (9.5 × 14.0 × 29.4) cm^3. The CEBs were tested in the longitudinal direction, giving a slenderness ratio of 3.1. The results of the CEBs with the dry densities 1980 kg/m^3 and 1820 kg/m^3 were observed: Fig. 10 and Table 2.

Although there was a difference in manufacturing technique (static compaction for CEBs and dynamic compaction for rammed earth), CEBs were chosen to replace rammed earth for the following reasons. First, they are manufactured in a mould and have fairly smooth surfaces, which helps solve the surfacing

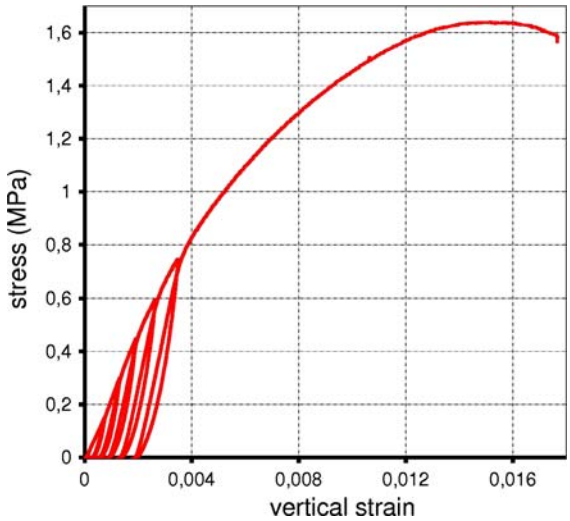

Fig. 10 Strain–stress curve of CEB sample, $d = 1980$ kg/m^3

Table 2 Calculation of the average modulus from equivalent CEB modulus

	Preload (MPa)					d (kg/m^3)
	0	0.06	0.12	0.22	0.4	
E_{up} (MPa)	185	260	310	390	480	$d_{up} = 1980$
E_{low} (MPa)	120	160	210	280	330	$d_{low} = 1820$
$<E>$ (MPa)	146	198	250	326	391	$<d> = 1900$

problem and the difficulties in contact with the press plate in the compression test. Secondly, they are fairly easy to manufacture and transport compared to rammed earth samples weighing over 200 kg, at the second scale. Thirdly, thanks to the manufacture of CEBs with double compaction, we can obtain almost homogenous samples.

Based on the CEB results, the calculation of $<E>$ in accordance with the formula (2) is presented in Table 2. These results will be discussed in Sect. 8.

7 In-situ measurements on structural elements (Fig. 1a)

7.1 Dynamic method principle

This method has already been used for seismic vulnerability assessment of existing buildings [16–18]. The mechanical characteristics of the materials were considered as well known and modified to fit to the modelling without any direct experiment to check their relevancy. Indeed the materials were well known material as concrete and brick masonry.

This method is also applied here basing on the relationship between the resonance frequency f of a sample with density ρ and its elastic constants:

$$f = F(\text{dimensions}, v)\sqrt{\frac{E}{\rho}} \tag{3}$$

where E is the elastic modulus and v is Poisson's ratio.

Therefore, this approach consists of 2 stages: in the first, the Eigen frequencies of in-situ walls are measured. In the second, models of these walls are constructed using the FEM with linear elasticity. Assuming the density and Poisson's ratio to be known, we can estimate the elastic modulus of the material from the frequencies measured.

7.2 Wall description

Dynamic measurements were taken twice. The first were taken in the summer (June) on walls number 1 and 2 (Fig. 3), 3 days after the construction of wall No. 1 and 18 days after construction of wall No. 2. The second measurements were taken 5 weeks later, also in the summer (July), on walls number 1, 2 and 3, when wall No. 3 had been completed for 18 days. The purpose of these two different measurements was to observe the elastic modulus change (if it existed) of these walls over time, or more accurately, with moisture content.

7.2.1 Measurement device

Accelerometer sensors with a sensitivity of μg (≈ 0.01 mm/s^2) were placed on the top and at the base of the wall (Figs. 11, 12). This sensor layout enabled us to measure the horizontal accelerations in two main axes and the torsional movement of the wall. Sensors 1, 3 and 6 measured accelerations in the transversal direction of the wall, while sensors 2, 4 and 5 measured the longitudinal accelerations. Sensors 1 and 2 were placed on the concrete foundation to see if the foundation vibrated with the wall. Sensors 3–6 were placed on the wall top to measure wall vibration.

The excitation mode consisted in applying light shocks (not quantified) to the wall with a hammer. Several configurations were made to excite the first modes of the wall. Figure 12 gives an example of

Fig. 11 Sensors disposition on top (left) and on base (right) of the wall for acceleration measurement

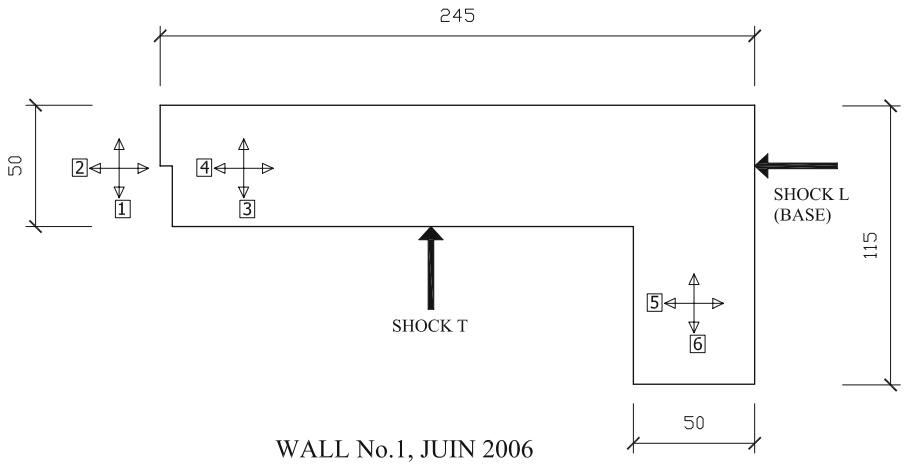

Fig. 12 Sensor layout on wall No. 1 and application of shocks. Sensors 1 and 2 are placed on the concrete foundation and sensors 3, 4, 5, 6 are placed on top of the wall

configurations on Wall No. 1: a shock T in the transversal direction and a shock L in the longitudinal direction of the wall.

7.2.2 In-situ frequency results

Examples of the frequencies of wall No.1 measured for a type T shock and a type L shock are presented in Figs. 13 and 14.

In the case of a T shock—Fig. 13, the result of sensor 6 gives the greatest resonance at 9.79 Hz with a magnitude of about 1 mm/s^2, indicating that the frequency of the first mode is 9.79 Hz, and that the vibration of the wall in the first mode is in the transversal direction (as there is no signal in sensor 5). With the same principle, from Fig. 14 we have the frequency of the second mode, 16.63 Hz, and the vibration is a torsional movement since both sensors 5 and 6 received similar signals at the same time. Then, the frequency determined for mode 3 is 23.38 Hz. The frequency of mode 4 was also determined but is not shown in these figures (>30 Hz).

Several measurements were taken and the representative values of the frequencies measured with their possible errors are presented in the fourth column of Table 3.

7.3 FEM modeling of the walls

The walls were modeled with the finite element method (using "solid elements", Fig. 15). When modeling, we assume that the material is isotropic and that Poisson's ratio is around 0.15 (a parametric study showed that this value does not significantly influence the results).

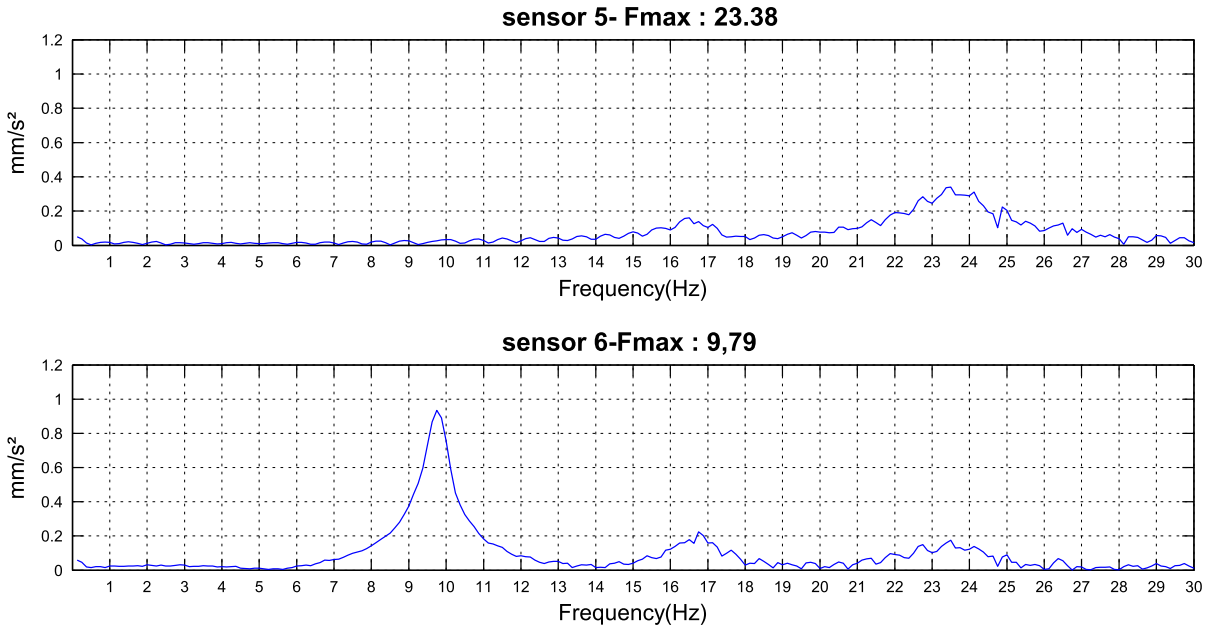

Fig. 13 Predominant frequencies measured by accelerometers for a T shock, wall No. 1, June (sensors 3 and 4 were saturated)

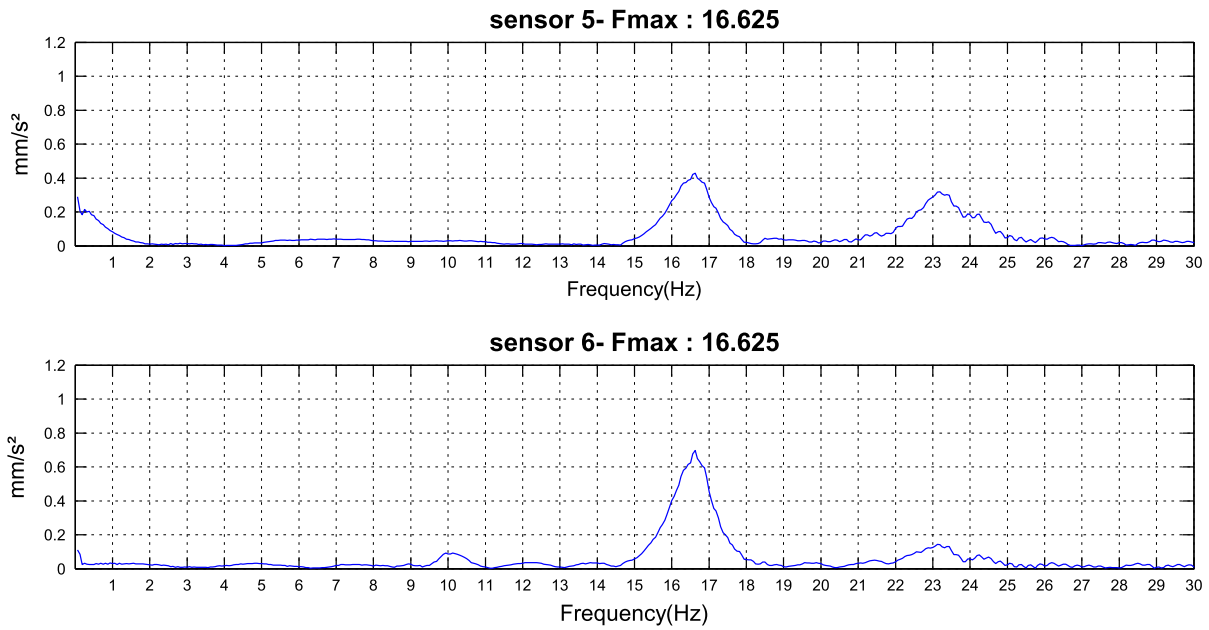

Fig. 14 Predominant frequencies measured by accelerometers for an L shock, wall No. 1, June (sensors 3 and 4 were saturated)

The in-situ measurements showed that the concrete base was much stiffer than the rammed earth wall. So we can consider that the rammed earth walls are embedded on the concrete base. For given dimensions, the Eigen frequencies depend solely on the density and elastic modulus of the material.

The material density was calculated from the dry density and moisture content. We assumed that the dry density of the in-situ walls was the same for all walls and equal to the density of the laboratory samples, in accordance with what was presented in section 5.2. The mean dry density obtained was 1900 kg/m^3.

Table 3 Frequencies obtained from in-situ measurements and modelling

Walls	Modes	f_{model} (Hz)	$f_{measured}$ (Hz) (%)	Difference (%)
Wall 1, June,	1	10.22	9.85 ± 1.0	3.7
w = 7%,	2	16.62	16.54 ± 1.2	−0.5
ρ = 2030 kg/m^3	3	22.76	23.38 ± 1.4	−2.6
E = 440 MPa	4	33.25	34.00 ± 1.5	−2.2
Wall 2, June,	1	10.94	10.90 ± 0.9	0.3
w = 4%,	2	16.48	16.60 ± 1.2	−0.7
ρ = 1980 kg/m^3	3	22.60	22.40 ± 1.4	0.5
E = 460 MPa	4	29.25	29.20 ± 1.4	0.2
Wall 1, July,	1	10.77	10.75 ± 0.9	0.2
w = 2.5	2	17.45	18.2 ± 1.6	−4.0
ρ = 1950 kg/m^3	3	24.01	24.0 ± 1.3	0.0
E = 470 MPa	4	35.06	36.5 ± 1.4	−3.9
Wall 2, July,	1	11.17	11.30 ± 0.8	−0.2
w = 2.5%,	2	16.83	17.10 ± 1.2	−1.6
ρ = 1950 kg/m^3	3	23.08	23.25 ± 0.9	−0.7
E = 470 MPa	4	29.87	30.5 ± 1.6	−2.1
Wall 3, July,	1	13.88	13.87 ± 1.4	0.0
w = 4%,	2	15.00	15.10 ± 1.3	−0.7
ρ = 1980 kg/m^3	3	24.34	25.25 ± 1.9	−3.6
E = 465 MPa	4	35.58	34.75 ± 0.6	2.4

Note: w and ρ are respectively the moisture content and density of the wall

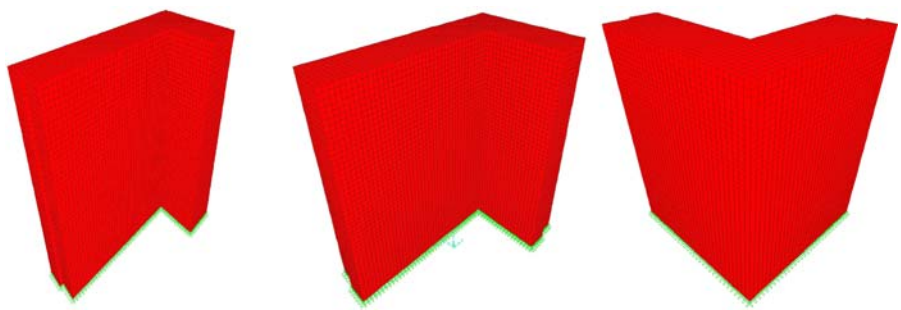

Fig. 15 FEM modeling of the walls. Left: wall No. 1; center: wall No 2 and right: wall No. 3

The change in the moisture content of the samples during their drying in the laboratory was recorded by several measurements at several moments. It is presented in the Fig. 16.

Let us assume that the change of the in-situ walls' moisture content is similar to that of the laboratory samples, although there are differences: the in-situ wall thickness is 10 cm greater, requiring longer drying; in-situ walls are exposed to direct sunlight, wind and rain while this is not the case of laboratory samples. The moisture content of the in-situ walls was estimated as follows:

- At the time of the first measurements (June): wall No. 1 had been finished for 3 days, therefore, following Fig. 16, we assumed that it had a moisture content of 7%, meaning that its density was 2030 kg/m^3. Wall No. 2 had been finished for 18 days, allowing us to assume a moisture content of 4%. Its corresponding density was 1980 kg/m^3.

The first three main vibration modes are presented in Fig. 17. The first mode is a vibration in the transversal direction of wall. The second is a torsional movement. In the third mode, the vibration is the width of 2 wall wings. These vibration aspects are completely appropriate with the in-situ signals received by the sensors (Figs. 13, 14). Thus the models confirm their good representation of the in-situ walls.

7.4 Determining the elastic modulus

Firstly, the model was tested with a modulus E_{trial}. The first Eigen frequency (called $f_{1\text{trial}}$) obtained from the model was noted.

From Eq. 3, we derive the following relationship:

$$\frac{f_{1\text{trial}}^2}{E_{\text{trial}}} = \frac{f_{1\text{measured}}^2}{E_{\text{measured}}} \tag{4}$$

$$\Rightarrow E_{\text{measured}} = \left(\frac{f_{1\text{measured}}}{f_{1\text{trial}}}\right)^2 E_{\text{trial}} \tag{5}$$

From Eq. 5, the modulus E_{measured} corresponding to the first in-situ frequency $f_{1\text{measured}}$ was determined.

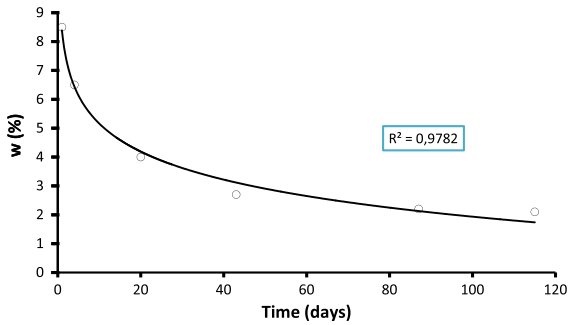

Fig. 16 Moisture content change of prism samples with time

Then the modulus was optimised to find a good correlation between the first four modelling frequencies and the in-situ frequencies. The modulus result obtained was presented in Table 3. The third column shows the corresponding Eigen frequencies of the models. The last column shows the difference between modelling frequencies f_{model} and in-situ frequencies f_{measured}. Figure 18 shows the comparison between the four first frequencies obtained from the modelling and those measured in-situ.

Based on the results presented in Table 3, we can draw the following conclusions:

- The FEM modeling gave results that correlated well with the in-situ measurements, confirming the acceptability of the assumptions used for the modeling. The difference between the dynamic measurement results themselves and between the modelling and in-situ measurement results did not exceed 4%.
- The moduli obtained for the walls were in the interval of 440–470 MPa. We can see a change of wall modulus with wall moisture content, Fig. 19. In the case of Wall No. 1, during the first measurements, 3 days after its construction it had a modulus of 440 MPa, which increased to 470 MPa five weeks later.

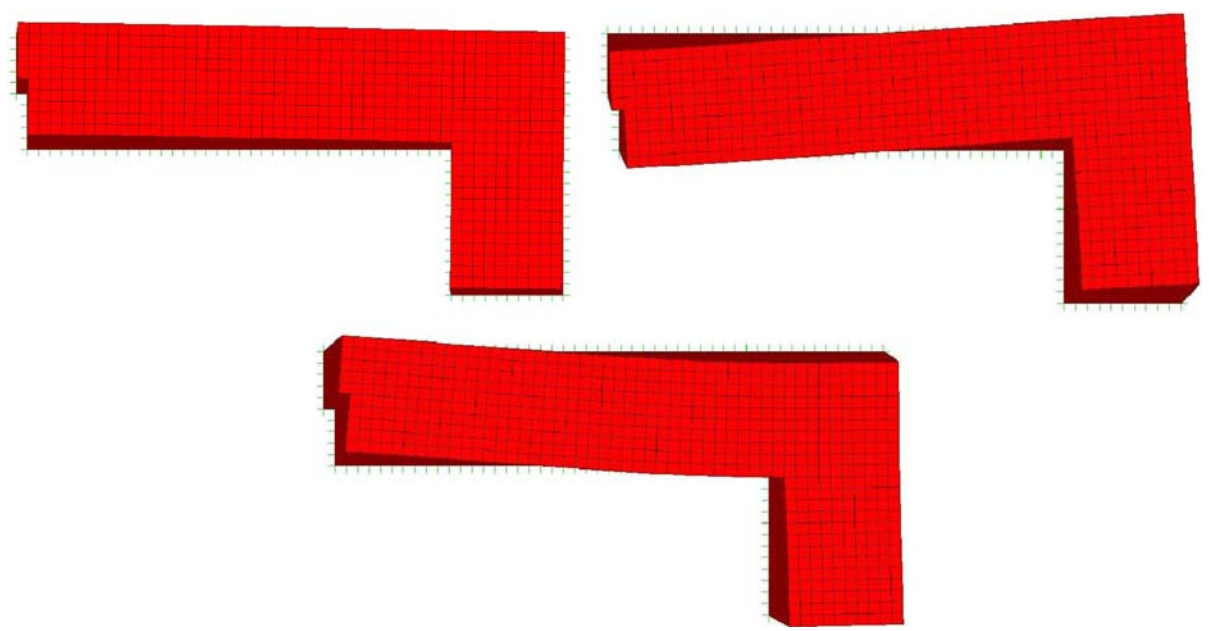

Fig. 17 First 3 vibration modes of wall No. 1, similar to those of wall No. 2. Upper-Left: mode 1; Upper-Right: mode 2 and Bottom: mode 3

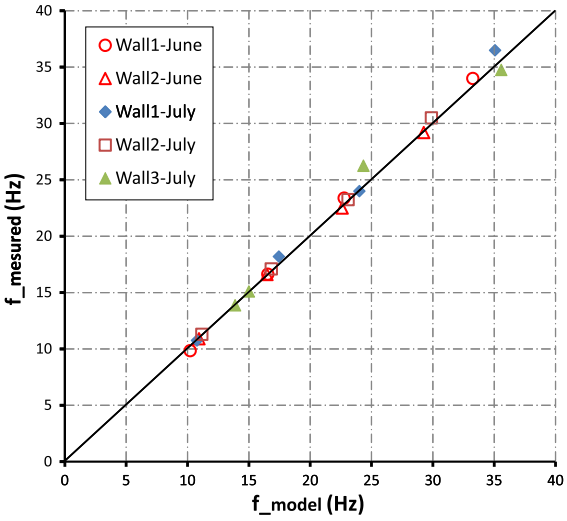

Fig. 18 Comparison between Eigen frequencies of models and those measured in-situ

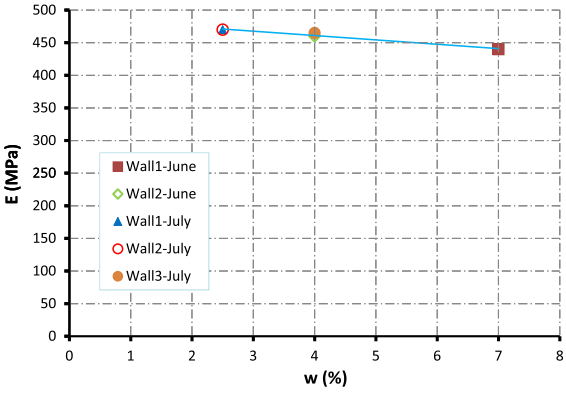

Fig. 19 Change of wall modulus depending on wall moisture content

8 Discussion of the results of the three approaches at three different scales

The summary of the results obtained with the three different approaches is presented in Fig. 20. We see that the result calculated from equivalent CEBs (third scale) is close to that obtained with the rammed earth RVEs tested in the laboratory (second scale). When the preload is low, the approach with CEBs gives a higher result, which may be due to a better surfacing of the CEBs.

The approach using in-situ dynamic measurements (first scale) gives a higher result than with the two other approaches, Fig. 20. On site, there is a preload

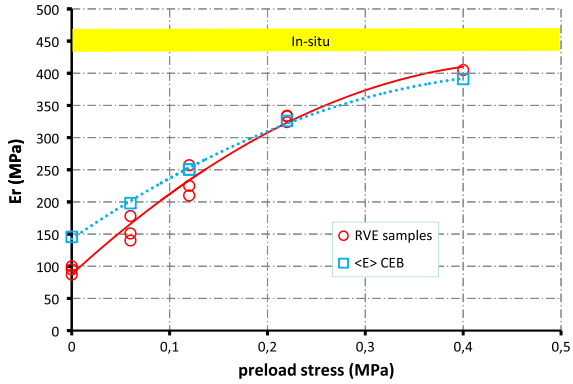

Fig. 20 Result summary for the three approaches

due to selfweight and wind, increasing from the base to the top. This preload is approximately 0.1 MPa at the base, however it is difficult to quantify it exactly. The approach using in-situ measurements gives results closer to the two laboratory approaches corresponding to a higher preload (0.4 MPa in this case).

The reasons that may account for the difference between the in-situ measurements and the laboratory tests are firstly that the adhesion between the rammed earth layer is considered perfect when modeling, whereas this is not the case in reality. Secondly, the behavior of the moisture in the in-situ walls may play a role. In the calculations, the walls are regarded as a continuum, "solid" medium, whereas in reality the moisture may behave differently in dynamics with the solid skeleton. One must also add that the water content in the walls is heterogeneous: the interior portions are more humid than the surface portions during drying. Thirdly, when modeling we did not take into account material anisotropy and the density gradient in each rammed earth layer, but at the macroscopic scale, this does not play an important role. Fourthly, the dynamic measurements were carried out in very small strains while in the case of laboratory static tests, the closure of micro-pores of the sample makes more important strain which cause the smaller moduli. Finally two moduli might be intrinsically different as concrete, where a coefficient is needed to link the dynamic and static response.

9 Conclusions and prospects

An experimental approach on three scales enables to determine mechanical characteristics of rammed

earth,which is characteristic of non-industrial material, with relatively simple models. For such materials, the difficulty of laboratory sample manufacturing requires in-situ measurements to validate laboratory results.

A dynamic approach on site (scale 1) in parallel with a "classic" static approach enable to determine the elastic modulus of rammed earth. After laboratory tests on rammed earth representative volume elements (RVEs-scale 2), a method to simplify sample manufacturing in the laboratory is proposed. The rammed earth samples are replaced with compressed earth blocks (CEBs-scale 3) with a similar density.

Measurements carried out with dynamic accelerometers (scale 1) are useful not only because they represent another approach to determine the rammed earth elastic modulus but also because they can pave the way for seismic calculations for rammed earth houses. They can be used to determine rammed earth dynamic characteristics, and to monitor the seismic vulnerability of existing rammed earth houses.

Given all of these factors, one future construction possibility would be to adapt ancestral techniques rather to than systematically abandon them. One would thus decide to shorten the production chain, which requires concentrating research on unusual criteria such as the validation of mason's know-how or of in-situ or even laboratory test procedures used to measure the performances of these materials, rather than on standardizing their composition.

Acknowledgement We wish to thank S. Courrier from the ENTPE for his assistance.

References

1. Morel JC, Mesbah A, Oggero M, Walker P (2001) Building houses with local materials: means to drastically reduce the environmental impact of construction. Build Environ 36:1119–1126
2. Bui QB, Morel JC, Venkatarama Reddy BV, Ghayad W (2008) Durability of rammed earth walls exposed for 20 years of natural weathering. Build Environ. doi: 10.1016/tj.buildenv.2008.07.001
3. Marcom A, Floissac L, Morel JC, How to assess the sustainability of building construction process (Submitted to Renew Energy)
4. Michel P, Poudru F (1987) Le patrimoine construit en terre en France métropolitaine. In: Colloque international Le patrimoine européen construit en terre et sa réhabilitation. Vaulx-en-Velin, France, pp 529–551
5. Dincyurek O, Mallickb FH, Numana I (2003) Cultural and environmental values in the arcaded Mesaorian houses of Cyprus. Build Environ 38:1463–1473
6. Hall M, Djerbib Y (2004) Rammed earth sample production: context, recommendations and consistency. Constr Build Mater 18:281–286
7. Lilley DM, Robinson J (1995) Ultimate strength of rammed earth walls with openings. Proc ICE: Struct Build 110(3):278–287
8. Maniatidis V, Walker P, Heath A, Hayward S (2007) Mechanical and thermal characteristics of rammed earth. In: International symposium on earthen sructures. Bangalore, pp 205–211
9. Jaquin PA, Augarde CE, Gerrard CM (2006) Analysis of historic rammed earth construction. Structural analysis of historical constructions. New Delhi, ISBN 972-8692-27-7
10. Maniatidis V, Walker P (2008) Structural capacity of rammed earth in compression. J Mater Civil Eng 20(3):230–238
11. Morel JC, Pkla A, Walker P (2007) Compressive strength testing of compressed earth blocks. Constr Build Mater 21:303–309
12. Bui QB, Hans S, Morel JC (2007) The compressive strength and pseudo elastic modulus of rammed earth. In: International symposium on earthen sructures. Bangalore, pp 217–223
13. Ward IM (1979) Mechanical properties of solid polimers, 2nd edn. Wiley-Interscience, 476 pp
14. Kouakou CH, Morel JC, Mechanical performance of nonindustrial building materials manufactured with clay as a natural binder (accepted by Applied Clay Science)
15. Pkla A (2002) Caractérisation en compression simple des Blocs de Terre Comprimée (BTC): application aux maconneries BTC-mortier de terre. PhD thesis, ENTPE Lyon, France, 229 pp
16. Hans S, Boutin C, Ibraim E, Roussillon P (2005) In-situ experiments and seismic analysis of existing buildings. Part I: Experimental investigations. Earthquake Eng Struct Dyn 34:1513–1529
17. Boutin C, Hans S, Ibraim E, Roussillon P (2005) In-situ experiments and seismic analysis of existing buildings. Part II: Seismic integrity threshold. Earthquake Eng Struct Dyn 34:1531–1546
18. De Sortis A, Antonacci E, Vestroni F (2005) Dynamic identification of a masonry building using forced vibration tests. Eng Struct 27:155–165